Journal of Power Sources 207 (2012) 86–90

Contents lists available at SciVerse ScienceDirect

Journal of Power Sources

journal homepage: www.elsevier.com/locate/jpowsour

Short communication

Improved performance of fuel cell with proton-conducting glass membrane

Zhigang Di[a], Haibin Li[b,*], Ming Li[a], Dali Mao[a], Xiaojing Chen[b], Ming Xiao[b], Jun Gu[c,*]

[a] School of Materials Science and Engineering, Shanghai Jiao Tong University, 800 Dong Chuan Road, Shanghai 200240, China
[b] Institute of Fuel Cell, School of Mechanical Engineering, Shanghai Jiao Tong University, 800 Dong Chuan Road, Shanghai 200240, China
[c] School of Physics, Nanjing University, Nanjing 210093, China

ARTICLE INFO

Article history:
Received 10 November 2011
Received in revised form 21 January 2012
Accepted 23 January 2012
Available online 31 January 2012

Keywords:
Proton-conducting glass
Glass membrane
Fuel cell
Membrane electrode assemblies

ABSTRACT

H_2/O_2 fuel cells equipped with proton-conducting Nafion®/phosphosilicate (NPS) glass membranes, which are prepared from phosphosilicate glass and a perfluorosulfonic acid polymer, are characterized, and their performances are improved step by step by using Nafion® resin as an adhesive, increasing operation temperature, adopting a thin-film pressure sensor, and reducing glass membrane thickness. Finally, the fuel cell with a 500 μm thick NPS glass membrane releases a peak power density of 207 mW cm^{-2} at 70 °C.

1. Introduction

Proton-exchange membrane fuel cells (PEMFCs) have attracted considerable attention as next-generation power sources for stationary and vehicular applications due to their environmental friendliness and high-energy utilization efficiency. Perfluorosulfonic acid polymer membranes, typically Nafion®, are characterized by high proton conductivity and good chemical stability, and therefore are widely used in PEMFCs as electrolytes. However, these membranes are very expensive and they suffer from swelling due to the adsorption of water, which lowers their fuel-cell efficiency.

Sol–gel derived inorganic proton conductors such as SiO_2 [1,2], Al_2O_3 [3], TiO_2 [3,4], P_2O_5–SiO_2 [5–9], and P_2O_5–TiO_2 [10] may offer very promising alternatives to polymeric membranes because of their low cost and high dimensional stability. Their proton conductivities can reach 10^{-2}–10^{-1} S cm^{-1} [4–10], which are comparable to that of Nafion® and are thus adequate for fuel-cell applications. Nevertheless, the power densities of fuel cells with proton-conductive glass membranes as electrolytes are still much lower than those of fuel cells based on Nafion® membrane. Using P_2O_5–SiO_2 and (phosphotungstic acid/phosphomolybdicacid) PWA/PMA–P_2O_5–SiO_2 membranes in fuel cells, Nogami et al. [11,12] obtained peak power densities of 6 mW cm^{-2} and 41.5 mW cm^{-2}, respectively. Matsuda et al. [13] attained a maximum power density of 30 mW cm^{-2} using phosphosilicate gel/polyimide composite membrane. Ioroi et al. [14] obtained a peak power density of 45 mW cm^{-2} using surface-modified porous glass with an attachment of —SO_3H onto the pore surface. Furthermore, Nogami et al. [15] prepared membrane electrode assemblies (MEAs) using the cold-pressed discs derived from phosphosilicate glass powder and H_3PO_4 as the binder, and attaining a peak power density of about 70 mW cm^{-2}. On the other hand, for intermediate-temperature fuel cells, Matsuda et al. [16,17] obtained maximum power densities of 38 mW cm^{-2} at 150 °C and 85 mW cm^{-2} at 130 °C using phosphosilicate gel/polyimide composite membrane and phosphosilicate hybrid gel/glass paper, respectively. In addition, our group has also demonstrated the utility of a sol–gel derived phosphosilicate glass membrane in a fuel cell, obtaining a peak power output of 20.8 mW cm^{-2} [8].

It is believed that a key issue is that sol–gel-derived glasses are inflexible and brittle, and thus cannot withstand the pressure required to press them into an MEA for favorable interface contact between the electrolyte and electrode. As a result, a high interface resistance arises, which is responsible for an undesirable power loss. Therefore, decreasing interface resistance is essential in order to improve the performance of a fuel cell with a glass membrane. On the other hand, it is well known that increasing the operating temperature and adopting a thinner electrolyte membrane could improve the performance of PEMFCs. It is expected that these methods will be effective for fuel cells with glass membranes.

Our group has recently prepared a Nafion®/phosphosilicate (NPS) glass membrane based on porous phosphosilicate glass and a perfluorosulfonic acid polymer by using a sol–gel process with a low-temperature hydrothermal treatment (below 150 °C), which could prevent thermal degradation of the organic component [18]. The incorporated highly proton conductive polyelectrolyte

* Corresponding author. Tel.: +86 21 34206249; fax: +86 21 34206249.
E-mail addresses: haibinli@sjtu.edu.cn (H. Li), junguca@nju.edu.cn (J. Gu).

0378-7753/$ – see front matter © 2012 Elsevier B.V. All rights reserved.
doi:10.1016/j.jpowsour.2012.01.136

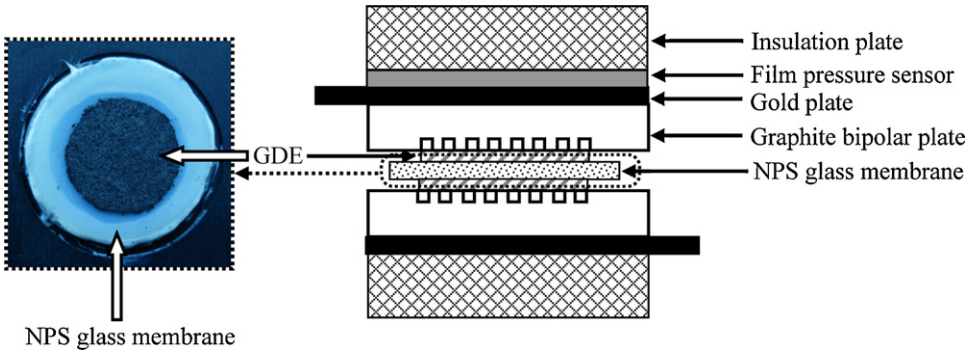

Fig. 1. Schematic illustration for assembling the fuel cell based on the NPS glass membrane, and optical image of MEA with the NPS glass membrane.

(Nafion®) could play a role in reducing the fuel permeation as a pore filler and in supplying additional proton conductive passes. The advantages of simple synthesis processes and low manufacturing costs make the NPS glass membrane very promising to substitute polymer electrolytes for the practical application in fuel cells. In the present work, the NPS glass membrane with 10 wt.% Nafion®, exhibiting a high proton conductivity of ca. 10^{-1} S cm^{-1} [18], was used for the preparation of the fuel cells. We showed that a single fuel cell equipped with the NPS membrane achieved a peak power density of 207 mW cm^{-2}. This density is much higher than the values of 6–85 mW cm^{-2} for the fuel cells constructed with proton-conducting glasses as electrolytes, reported previously [8,11–17].

2. Experimental

2.1. Materials

$Si(OC_2H_5)_4$ (TEOS, Sinopharm), H_3PO_4 (85% aqueous solution, Sinopharm), and Nafion® perfluorinated ion-exchange resin (10 wt.%, DuPont) were used without further purification.

2.2. Preparation of NPS glass membrane

The NPS glass membrane was prepared by a sol–gel method as reported previously [18]. Briefly, a mixture of $Si(OC_2H_5)_4$ (TEOS), deionized water, and hydrochloric acid in a molar ratio of $1{:}4{:}4 \times 10^{-3}$ (TEOS:H_2O:HCl) was initially prepared and stirred for 30 min at room temperature. Then, phosphoric acid solution and Nafion® resin in molar ratios of 3:7 (H_3PO_4:TEOS) and 1:9 (Nafion®:TEOS) were slowly added to the above mixture and stirring was continued for 20 min. The obtained transparent solution was then transferred to a Teflon® vessel and left to stand at room temperature until gelation occurred. Teflon vessels with xerogels were introduced into a drying box. The gel was then hydrothermally treated at 150 °C for 24 h, and a water vapor at a pressure of 1 atm was maintained within the drying box by providing an excess of deionized water. After these procedures, the NPS glass membrane was obtained. The thickness of the membrane can be controlled by changing the solution amount cast into the vessel.

2.3. Preparation and test of fuel cell with the NPS glass membrane

Gas-diffusion electrodes (GDEs) with a Pt loading of 0.5 mg cm^{-2} were prepared by spraying the catalyst ink onto wet-proofed Toray carbon paper. Using a process called Method A, a sandwiched MEA with a circular 0.8 cm diameter active region was made by attaching the GDEs onto the glass membrane, and then the MEA held between two graphite bipolar plates was placed between two gold plates. As an alternative called Method B, the MEA with the same active region was made by attaching the GDEs onto the glass membrane using Nafion® resin (10 wt.% solution in a mixture of lower aliphatic alcohols and water) as an adhesive, and then the MEA sandwiched between two graphite bipolar plates was placed between two gold plates. In addition, Method B was improved, in which a thin-film pressure sensor (Flexiforce® A401, Tekscan Inc.) as an additional part was inserted between the gold plate and the insulation plate for assembling the fuel cell. A schematic illustration for assembling the fuel cell is shown in Fig. 1.

The H_2/O_2 fuel cells were fueled with hydrogen supplied to the anode and oxygen supplied to the cathode, each at a pressure of 1 atm. The flow rates and humidification of the gases and the temperature of the cells were controlled by a fuel-cell testing system (FC 5100, CHINO Corp.). The gas flow rates of H_2 and O_2 were 30 sccm and 60 sccm, respectively. Electrochemical data, including polarization curves and electrochemical impedance spectroscopy (EIS), were performed and collected by an Impedance/Gain-Phase Analyzer (SI1260, Solartron) and an Electrochemical Interface (SI1287, Solartron). The amplitude of the AC signal was 10 mV and the scanning frequency was typically varied from 0.1 Hz to 1 MHz. The impedance spectra of the glass membrane based H_2/O_2 fuel cell were measured at 0.4 V.

2.4. Characterization

Scanning electron microscopy (SEM) image of the NPS glass membrane painted with Nafion® solution (10 wt.% solution) was obtained on a field-emission SEM (NOVA, NanoSEM 230) equipped with energy dispersive X-ray spectroscopy (EDS) (INCA X-Max 80, Oxford Instruments). EDS was used to characterize the composition distribution of the Nafion infiltrated into the NPS glass membrane.

3. Results and discussion

3.1. Effect of MEA preparation process

The NPS glass membrane was prepared by a hydrothermal-assisted sol–gel method. A photo of the MEA which are based on the NPS glass membrane is shown in Fig. 1. Polarization and power output curves were recorded to assess the fuel cell performance and their improvement, as shown in Fig. 2. The fuel cells operating at room temperature, which are prepared with Method A and Method B, released maximum output powers of 14.4 and 45.4 mW cm^{-2}, respectively. Obviously, the cell using Method B showed much better performance than that with Method A. The large discrepancy in output power should be due to the difference of internal resistance including ohmic and electrode resistances for both fuel cells. An impedance analysis of the fuel cells was carried out and impedance spectra are shown in Fig. 3. The intercept in the high-frequency domain on the real axis represents ohmic resistance (R_Ω), and it is mainly ascribed to the membrane

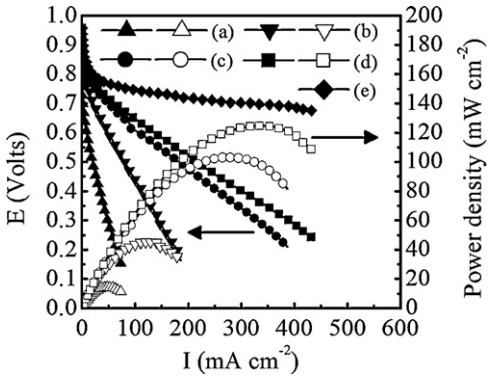

Fig. 2. *I–V* and power density curves of fuel cells, which are based on the NPS glass membrane with a thickness of 800 μm. The performance of a fuel cell operating at room temperature, which was prepared by Method A, is shown. The improved performances of fuel cells operating at room temperature by using Nafion® resin as an adhesive (b), operating at 70 °C by increasing operation temperature (c), and operating at 70 °C by adopting a thin-film pressure sensor (d) are also given, which were prepared by Method B. Curve (e), *iR-correction* result for the initial measurement of the fulel cell operating at 70 °C with the thin-film pressure sensor.

resistance and interfacial resistance between membrane and electrodes, both of which are protonic resistances. The semicircle in the low-frequency domain represents the electrode resistance, which is mainly charge–transfer resistance (R_c) on the anode and cathode, with the main contribution being the cathode oxygen reduction reaction (ORR) process.

The cell prepared using Method A had an ohmic resistance of 2.3 Ω cm^2 and a charge–transfer resistance of 2.7 Ω cm^2, while the cell prepared using Method B gave an ohmic resistance of 1.3 Ω cm^2 and charge–transfer resistance of 2 Ω cm^2. Compared to that of Method A, ohmic resistance and charge–transfer resistance for the fuel cell using Method B were evidently reduced. The NPS glass membrane could not endure hot pressing to assemble the MEA and the fuel cell, due to the fact that hot pressing would crush the NPS glass. For the cell with Method A, the high interfacial resistance developed with very poor interfacial contact between the NPS glass and the electrodes, and thus it gave rise to a large ohmic resistance. In contrast, due to the fact that the Nafion® resin can provide better adhesion and a stronger binding force

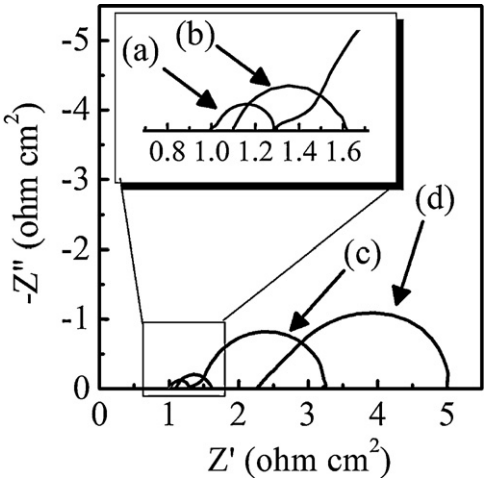

Fig. 3. Impedance spectra of fuel cells measured at 0.4 V, which are based on the NPS glass membranes with a thickness of 800 μm. The impedance spectrum of a fuel cell operating at room temperature, which was prepared by Method A, was shown. Impedance spectra of fuel cells operating at room temperature by using Nafion® resin as an adhesive (b), operating at 70 °C by increasing operation temperature (c), and operating at 70 °C by adopting a thin-film pressure sensor (d) are also given, which were prepared by Method B.

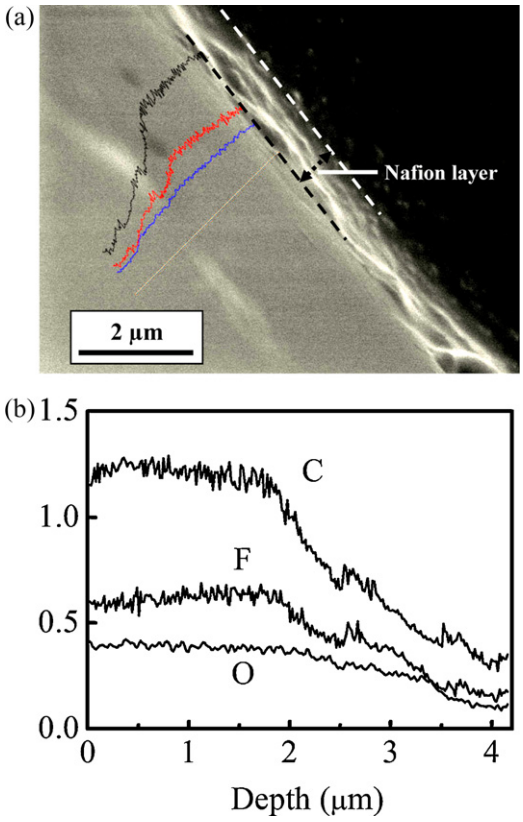

Fig. 4. Cross-sectional SEM image (a) and corresponding EDS composition profiles (b) of a Nafion®-painted NPS glass membrane.

between the glass membrane and the electrodes, better interfacial contact could be formed, leading to the reduction of interfacial resistance. In addition, it is well known that creating the so-called triplephase boundaries, in which the protonic electrolyte, catalytic particles, and reactants are in close contact with each other, is critical in reducing charge–transfer resistance. The introduction of a Nafion® layer between the rigid NPS glass and the electrodes could achieve better triplephase boundaries, leading to the reduction of charge–transfer resistance. Thereby, the utilization of Nafion® resin by Method B leads to the reduction of both ohmic resistance and charge–transfer resistance of the fuel cell, and thus the increased output power was obtained.

Fig. 4 shows cross-sectional SEM image and corresponding EDS composition profiles of a Nafion®-painted NPS glass membrane. As shown in Fig. 4(a), the Nafion® layer attached on the NPS glass membrane has a thickness of 800 nm. On the other hand, EDS composition profiles in Fig. 4(b) give the distributions of C, O, and F elements within the NPS glass membrane. The sectional distribution of the Nafion® infiltrated into the NPS glass membrane is determined by checking F species. In Fig. 4(b), the F species gradually decreased from the surface toward the interior, and tend to reach a constant level onto the depth of ca. 4 μm. These results suggest that the Nafion® could infiltrate into the surface layer of the NPS glass membrane in an infiltration depth of ca. 4 μm. The Nafion® was introduced to improve interface adhesion between the glass membrane and the electrodes. On the other hand, the introduction of the Nafion should be also helpful for promoting proton conduction within the surface layer of the glass membrane, and for reducing fuel crossover in some extent.

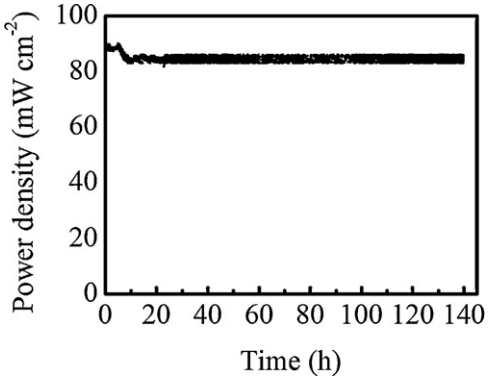

Fig. 5. Output power as a function of time under a cell votage of 0.5 V for 140 h.

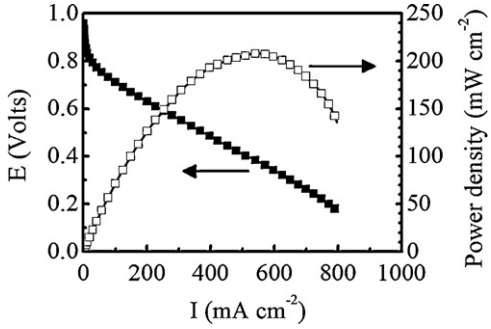

Fig. 6. *I–V* and power density curves of fuel cell with a 500 μm thick NPS glass membrane oprating at 70 °C, which was prepared by Method B.

3.2. Effect of operating temperature

Increasing the operation temperature has been considered an effective approach for improving fuel cell performance. As expected, the fuel cell performance shown in Fig. 2 increased dramatically from 45.4 to 103 mW cm^2 with increasing operation temperature from 25 to 70 °C. The resultant impedance spectra at both temperatures are shown in Fig. 3. It is observed that ohmic resistance decreased slightly from 1.3 to 1.1 Ω cm^2, while electrode resistance decreased significantly from 2 to 0.5 Ω cm^2 when the temperature increased from 25 to 70 °C. Ohmic resistance decreased as the temperature increased, which may have been due to an increase of the membrane conductivity, as reported in the literature [18], in which proton conductivities of ca. 0.07 S cm^{-1} at 30 °C and ca. 0.1 S cm^{-1} at 70 °C under 70% relative humidity were given. According to electrochemical reaction kinetics, increasing the temperature could increase the rate of the electrode reaction. Electrode resistance results mainly from charge–transfer resistance and is a direct function of the slow ORR kinetic at the cathode which becomes faster as the temperature increases [19]. In addition, the increased operation temperature also could improve the mass-transfer process, resulting in improved performance.

3.3. Effect of assembly pressure

To reduce interfacial resistance, assembly pressure should be increased as high as possible. For the present study, the NPS glass membrane used could not endure hot pressing to assemble the MEA due to its friability, so that the applied assembly pressure is critical for the reduction of interfacial resistance. In order to accurately control the assembly pressure, and to increase it as high as possible under the prerequisite conditions without crushing the NPS glass, a thin-film pressure sensor was inserted between the gold plate and the insulation plate, as shown in Fig. 1.

During the fuel cell assembly, progressively increasing force was applied, and a maximum contact pressure of 4.5 N was used to perform measurements due to the fact that higher pressure tends to crush the glass membrane. As shown in Fig. 2, an increased output power of 124.7 mW cm^{-1} for the fuel cell with the thin-film pressure sensor was obtained at 70 °C, compared to the value of 103 mW cm^{-1} at 70 °C for that assembled on the basis of operator experience, without the thin-film pressure sensor. Meanwhile, Fig. 3 shows that the ohmic resistance and electrode resistance decreased from 1.1 and 0.5 Ω cm^2 to 1 and 0.3 Ω cm^2, respectively, by the adoption of the thin-film pressure sensor.

In order to assess the stability of the NPS glass membrane under fuel-cell conditions, the longevity experiment was carried out. Fig. 5. gives the stability of output power as a function of time under a cell votage of 0.5 V. The assembling configuration and operating condition of the fuel cell for stability measurement are identical to those of the fulel cell with the thin-film pressure sensor in Fig. 2. After an initial drop from ca. 90 to 85 mW cm^{-2}, during the continuous measurement up to 140 h, the fuel cell showed remarkable stability. The result demonstrates the high stability of the NPS glass membrane under fuel cell conditions. The reason for the drop in output power in the first few hours is still not clear. Further study is definitely required.

3.4. Effect of the NPS glass thickness

The *iR-correction* is given from the following formula: *iR-correction* = $E - iR_\Omega$, where E is the measured cell voltage, i is the current density, and R_Ω is the ohmic resistance determined from impedance spectrum. The *iR-correction* result for the initial measurement of the fulel cell operating at 70 °C with the thin-film pressure sensor is shown in Fig. 2 as curve (e).

In comparison to conventional PEMFCs using the polymer electrolyte membranes, whose thicknesses range from the teens to 180 μm, performance limitations were believed to be related to membrane resistance of the NPS glass membrane, which is expected to be fairly large due to the utilization of an 800 μm thick glass membrane. Decreasing the NPS glass membrane thickness could therefore be expected to increase the performance. Thus, we constructed a fuel cell by using 500 μm thick NPS glass. As shown in Fig. 6, the fuel cell operating at 70 °C gave an open-circuit voltage of 0.96 V, and released a peak power density of 207 mW cm^{-2}, which is evidently greater compared to that with an 800 μm thick

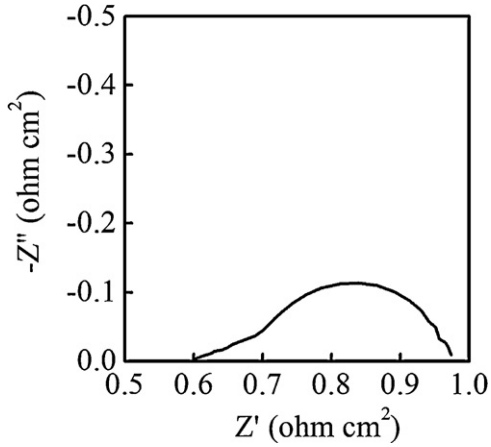

Fig. 7. Impedance spectra of fuel cells measured at 0.4 V, which are based on the NPS glass membranes with a thickness of 500 μm.

glass membrane. In addition, this value is much higher than the peak power density of ca. 6–85 mW cm^{-2} previously reported for fuel cells utilizing glass electrolytes [8,11–17]. Fig. 7 shows that the ohmic resistance decreased to 0.6 Ω cm^2 by using the thinner 500 μm thick NPS glass membrane to substitute the 800 μm thick membrane.

4. Conclusion

In this study, the performance of a fuel cell equipped with a proton-conducting NPS glass membrane was improved step by step. Finally, the H_2/O_2 single fuel cell with a 500 μm thick NPS glass membrane released a peak power density of 207 mW cm^{-2}. Based on this promising output power, such low-cost glass membranes may possibly be used as novel proton-exchange membranes in fuel cells. Another possible application of this kind of membrane might be in hydrogen and humidity sensors.

Acknowledgements

This work was supported by the National High-Tech R&D Program (863 Program) (Grant No. 2009AA05Z113), the International Science & Technology Cooperation Program of Ministry of Science & Technology (Grant 2008DFA51200), the National Natural Science Foundation of China (Grant No. 50672058).

References

[1] M. Nogami, R. Nagao, C. Wong, J. Phys. Chem. B 102 (1998) 5772–5775.
[2] Y. Daiko, T. Akai, T. Kasuga, M. Nogami, J. Ceram. Soc. Jpn. 109 (2001) 815–817.
[3] F.M. Vichi, M.T. Colomer, M.A. Anderson Electrochem, Solid State Lett. 2 (1999) 313–316.
[4] M.T. Colomer, Adv. Mater. 18 (2006) 371–374.
[5] M. Nogami, R. Nagao, C. Wong, T. Kasuga, T. Hayakawa, J. Phys. Chem. B 103 (1999) 9468–9472.
[6] S. Suzuki, Y. Nozaki, T. Okumura, M. Miyayama, J. Ceram. Soc. Jpn. 114 (2006) 303–307.
[7] S.P. Tung, B.J. Hwang, J. Mater. Chem. 15 (2005) 3532–3538.
[8] H. Li, D. Jin, X. Kong, H. Tu, Q. Yu, F. Jiang, Micropor. Mesopor. Mater. 138 (2011) 63–67.
[9] A. Matsuda, H. Honjo, M. Tatsumisago, T. Minami, Chem. Lett. 27 (1998) 1189–1190.
[10] M. Yamada, D.L. Li, I. Honma, H.S. Zhou, J. Am. Chem. Soc. 127 (2005) 13092–13093.
[11] Nogami, H. Matsushita, Y. Goto, T. Kasuga, Adv. Mater. 12 (2000) 1370–1372.
[12] T. Uma, M. Nogami, Anal. Chem. 80 (2008) 506–508.
[13] A. Matsuda, N. Nakamoto, K. Tadanaga, T. Minami, M. Tatsumisago, Solid State Ionics 162–163 (2003) 247–252.
[14] T. Ioroi, K. Kuraoka, K. Yasuda, T. Yazawa, Y. Miyazaki, Electrochem. Solid-State Lett. 7 (2004) A394–A396.
[15] M. Nogami, K. Tanaka, T. Uma, Fuel Cells 9 (2009) 528–533.
[16] N. Nakamoto, A. Matsuda, K. Tadanaga, T. Minami, M. Tatsumisago, J. Power Sources 138 (2004) 51–55.
[17] T. Tezuka, K. Tadanaga, A. Matsuda, A. Hayashi, M. Tatsumisago, Electrochem. Commun. 7 (2005) 245–248.
[18] F. Jiang, Z. Di, H. Li, H. Tu, Q. Yu, J. Power Sources 196 (2011) 1048–1054.
[19] Y. Tang, J. Zhang, C. Song, H. Liu, J. Zhang, H. Wang, S. Mackinnon, T. Peckham, J. Li, S. McDermid, P. Kozak, J. Electrochem. Soc. 153 (2006) A2036–A2043.